Osteoarthritis and Cartilage 22 (2014) 1936–1946

Osteoarthritis and Cartilage

Defective autophagy in chondrocytes with Kashin-Beck disease but higher than osteoarthritis

C. Wu †, J. Zheng †, X. Yao †, H. Shan ‡, Y. Li §, P. Xu ||, X. Guo † *

† School of Public Health, Xi'an Jiaotong University Health Science Center, Key Laboratory of Environment and Genes Related to Diseases, Ministry of Education, Key Laboratory of Trace Elements and Endemic Diseases, Ministry of Health, Xi'an, Shaanxi 710061, China
‡ Department of Respiratory Medicine, Second Affiliated Hospital, Xi'an Jiaotong University, Xi'an 710004, China
§ Department of Ankle Joint, Hong Hui Hospital, Xi'an Jiaotong University Health Science Center, Xi'an 710054, China
|| Department of Joint Surgery, Hong Hui Hospital, Xi'an Jiaotong University Health Science Center, Xi'an 710054, China

ARTICLE INFO

Article history:
Received 31 January 2014
Accepted 18 August 2014

Keywords:
Kashin-Beck disease
Osteoarthritis
Autophagy
Cell death
Mitochondria

SUMMARY

Objective: This study was undertaken to monitor autophagy in chondrocytes with Kashin-Beck disease (KBD) and osteoarthritis (OA).

Methods: The identification and quantification of autophagy were morphologically visualized by transmission electron microscopy (TEM), together with immunohistochemical localization of Beclin1 and LC3 in cartilage, and immunoblotting of cellular Beclin1, LC3 and p62/SQSTM1 in the normal, KBD and OA groups. Sequentially, regulated-autophagy genes (ATG) were analyzed by IPA software and validated by quantitative real-time polymerase chain reaction (qRT-PCR). Cytotoxicity of cell death was measured by fluorescence detection and flow cytometry (FCM). The co-localization and measurement of autophagy and mitochondria/reactive oxygen species (ROS) were carried out.

Results: KBD chondrocytes exhibited a variety of abnormal cellular contents including nuclei, mitochondrial, glycogen deposits and microfilaments, and OA chondrocytes mainly presented swelled endocytoplasmic reticulum (ER). Beclin1 and LC3 were reduced both in KBD and OA compared with normal controls; however, the two proteins and p62 in KBD were in a higher level than OA. Simultaneously, KBD chondrocytes showed 45 genes that were different from normal controls and 92 genes different from OA, whose functions were mainly involved in cell morphology, cellular functions, cell death and survival. Autophagy was negatively correlated with apoptosis in the three kinds of chondrocytes, and the rates decreased when autophagy was induced by rapamycin. Similarly, KBD and OA chondrocytes showed lower autophagy and higher ROS production compared with the normal chondrocytes.

Conclusion: Autophagy was defective in KBD chondrocytes, but it was higher than in OA. The insufficient autophagy may be associated with apoptosis and mitochondrial change in the pathogenesis of KBD and OA.

Introduction

Osteoarthritis (OA) is the most common bone-joint disease, characterized by progressive destruction of articular cartilage, synovial inflammation, severe pain, impaired movement and ultimately disability. Kashin-Beck disease (KBD) is a deformed, endemic osteochondropathy which occurs commonly in children and can lead to growth retardation, secondary osteoarthrosis and disability in its advanced stages[1,2]. KBD displays similar clinical characteristics and pathologic alterations as OA, such as degradation of the matrix, cartilage degeneration and chondrocyte apoptosis[3,4]. KBD also shows different manifestations of cartilage damage including excessive cell de-differentiation, focal cell necrosis in the growth plate and articular cartilage, and significant alterations in chondrocyte phenotype[5]. In addition, KBD chondrocytes present mitochondria dysfunction[6] and altered gene and protein expression profiles[7,8]. The autophagic response allows terminally differentiated chondrocytes to survive the gross impairment of growth plates resulting from harsh disturbances[9]. The terminal chondrocytes undergo autophagy prior to the induction of osteogenesis[10]. On the other hand, autophagy appears to

* Address correspondence and reprint requests to: X. Guo, Xi'an Jiaotong University, Health Science Center, No. 76 Yanta West Road, Xi'an, Shaanxi 710061, China. Tel: 86-29-82655091; Fax: 086-029-82655032.
E-mail addresses: xj.cy.69@stu.xjtu.edu.cn (C. Wu), 164857627@qq.com (J. Zheng), yaox_iao@126.com (X. Yao), yaosha1860@stu.xjtu.edu.cn (H. Shan), tongrenly@163.com (Y. Li), sousou369@163.com (P. Xu), guox@mail.xjtu.edu.cn (X. Guo).

http://dx.doi.org/10.1016/j.joca.2014.08.010
1063-4584/

decline with age and counteracts the aging process[11]. Loss of autophagy progressive with aging causes accumulation of damaged mitochondria, which enhances cell death and inflammation, resulting in OA[12].

Evidence is accumulating that autophagy has protective and survival-promoting functions in arthritic cartilage, while loss or derangement of autophagy is implicated as a mechanism contributing to OA[13]. Autophagy is a transient stage in the maturation of growth plate chondrocytes that is regulated by the activities of adenosine 5'-monophosphate-activated protein kinase (AMPK) and mammalian target of rapamycin (mTOR)[14]. Chondrocytes embedded in the external matrix in the growth plate and articular cartilages survive in an almost avascular and hypoxic microenvironment. The transcription factor hypoxia-inducible factor 1 (HIF-1) promotes the onset of autophagy in chondrocytes[15]. Conversely, HIF-2α level is high in OA cartilage and suppresses chondrocyte autophagy, thereby promoting chondrocyte apoptosis[16]. The term "chondroptosis" was defined as the type of cell death present in articular cartilage, which includes classical apoptosis and autophagy[17]. Autophagy is an intermediate stage in the chondrocyte life cycle that permits the cells to transform into a mature phenotype prior to their elimination by apoptosis[18].

In this study, firstly, we present autophagy level of human KBD and OA chondrocytes compared with the normal, involving cellular morphological changes, proteins expression level and RNA expression analysis. Then, we examined whether autophagy was associated with cell death and mitochondrial function in KBD and OA chondrocytes by simultaneously measuring the fluorescence markers.

Methods

Subject information and inclusive and exclusive criteria

Human articular cartilages were collected from six normal people who had suffered accidents (three females/three males, 55.0 ± 6.1 years old), six KBD patients (four females/two males, 58.2 ± 4.5 years old) and six OA patients (three females/three males, 59.3 ± 4.8 years old) who were undergoing total knee replacement surgery. KBD patients were diagnosed according to the Diagnosing Criteria of Kashin-Beck Disease in China (WS/T 207-2010). All of the subjects were excluded rheumatoid arthritis and the genetic bone and cartilage diseases. This investigation was approved by the Human Ethics Committee of Xi'an Jiaotong University. Each donor signed an informed consent.

Cartilage tissue collection and chondrocyte culture

The articular cartilages were resected from the bones and were rinsed in phosphate buffered saline (PBS) with antibiotics (penicillin and streptomycin). To isolate chondrocytes, the cartilage tissues were cut into 5 mm^3 slices, and incubated with trypsin at room temperature for 30 min. After removing the trypsin solution by PBS washing, the tissue slices were treated for 12–16 h with type II collagenase. Then the cells were harvested and cultured at 37°C in 5% CO_2 in DMEM/F-12 (1:1) supplemented with 10% (v/v) fetal calf serum (HyClone, Logan, Utah, USA), 100 units/mL penicillin and 100 μg/mL streptomycin. In order to obtain a sufficient amount of cells to meet the requirements of all the experiments, first-passage cells were used in experiments.

Transmission electron microscopy (TEM) for viewing chondrocytes in cartilages

The cartilage tissue slices were fixed with ice-cold 3% glutaraldehyde in 0.1M cacodylate buffer, postfixed in osmium tetroxide and embedded in Epon epoxy resin. Ultrathin sections were cut, stained with 0.1% lead citrate and 10% uranyl acetate, and viewed with a Hitachi 7650 transmission electron microscope.

Immunohistochemical localization of Beclin1 and LC-3 in cartilage

Paraffin-embedded cartilage sections were first deparaffinized in xylene and rehydrated in graded ethanol series and water. Sections were treated with 3% hydrogen peroxide for 10 min, washed with PBS and incubated in 10 M urea solution and trypsin at 37°C for 20 min to unmask antigen. After blocking with 5% goat serum for 20 min at room temperature, Beclin1 (Epitomics, Burlingame, CF, USA. rabbit monoclonal antibody) and LC3 (Cell Signaling Technology, Boston, MA, USA. rabbit monoclonal antibody) antibody (1:50 dilution) as well as negative control IgG were applied and incubated overnight at 4°C. After washing with PBS, sections were incubated using the SAP kit (Zhongshan Jinqiao, Guangzhou, China). The substrate 3,3′-diaminobenzidine (DAB) was added to stain sections with hematoxylin counterstaining. Finally, sections were dehydrated and mounted under cover slips. Beclin1 and LC3 localization in each cartilage zone was assessed systematically by counting the rate of positive cells.

Western blotting for endogenous Beclin1, LC-3 and p62/SQSTM1

Chondrocytes were lysed using radio immunoprecipitation assay (RIPA) lysis buffer with phenylmethylsulfonyl fluoride (PMSF), protease inhibitor, phosphatase inhibitor, and the protein concentration of the lysate was measured using the BCA protein assay kit (Thermo Fisher Scientific, Boston, MA, USA). Proteins were separated by SDS-polyacrylamide gelelectrophoresis (SDS-PAGE) and transferred to polyvinylidenedifluoride (PVDF) membranes. The membranes were blocked in nonfat dry milk solution and incubated overnight at 4°C with Beclin1 (1:750), LC3 (1:1000) and p62/SQSTM1 (1:1000) primary antibody dilution buffer and then incubated with horseradish peroxidase (HRP)-conjugated anti-rabbit IgG (1:3000) for 2 h. Afterwards, the membranes were developed using the enhanced chemiluminescence substrate LumiGLO (Millipore, Bedford, MA, USA) and exposed to X-ray film. The bands were analyzed with Gel-Pro Analyzer 4.0.

Identifying a core autophagic gene set and analyzing associated biological information

The microarray data was from oligonucleotide microarray analysis of KBD and normal chondrocytes implemented by Weizhuo Wang, *et al.*[7]. A human autophagy database including 229 autophagy genes (ATG) was downloaded from the Public Research Centre for Health (http://autophagy.lu/clustering/index.html). First, the two lists were compared to determine genes associated with autophagy expressed in chondrocytes. Then, these genes and ratios (KBD/control) were uploaded to IPA (Ingenuity® Systems, http://www.ingenuity.com) software, setting *n*-fold change equal to 1.5 (up-regulated expression) or 0.67 (down-regulated expression) and executing sequential analysis of functions, pathway, networks, upstream regulators and molecules. The microarray data from KBD and OA chondrocytes (implemented by Chen Duan) were analyzed as above[19]. In the microarray experiment, there were four sample pairs of KBD patients and the control cases (the normal or OA patients) in each comparison, which matched age and sex.

The genes selected from the above two analyses were further evaluated using quantitative real-time polymerase chain reaction (qRT-PCR) amplification to validate the oligonucleotide array data. Total RNA of chondrocytes was extracted using trizol regent and reverse-transcribed into cDNA. Steady-state mRNA levels were

quantified by two step SYBR Green RT-PCR using iCycler iQ5. The relative amount of each transcript was normalized against the amount of the GAPDH transcript. Relative fold change of each individual gene was calculated using the comparative Ct equation. The set of following genes were analyzed: BAK1 (NM_001188), BAX (NM_138764), BCL2 (NM_000633), BNIP3 (NM_004052) and BNIP3L (NM_004331). The oligonucleotide primers information was showed in Supplementary material Table 1.

Autophagy and cell death of chondrocytes

The regulation of autophagy and cell death at the cellular level was assayed by the autophagy/cytotoxicity dual staining kit (Abcam, Cambridge, UK) using monodansylcadaverine (MDC) and propidium iodide (PI). Cells were seeded in 24-well plates with 5×10^5 cells/well. When the density of the cells reached 80%–90% confluence, plates were centrifuged and the supernatants aspirated, then cells were stained with PI and MDC solution using the same protocol. Then, the cells were analyzed with a fluorescence plate reader (MDC, 335 nm/512 nm; PI, 536 nm, 617 nm) and images were obtained immediately by fluorescence microscopy. In addition, chondrocytes were treated with the autophagy inducer rapamycin (Sigma-R8781) at 1 mM for 48 h. The apoptosis rate was measured by flow cytometry (FCM) using the Annexin V-FITC/PI apoptosis detection kit (Becton Dickinson, San Jose, CA, USA).

Colocalization of autophagy with mitochondria or reactive oxygen species (ROS)

MDC and MitoTrackerprobes (Invitrogen, Spartak Calder, CF, USA) were used in double staining to label intracellular autophagy and mitochondria, respectively, as well as MDC and 2′,7′-dichlorofluorescin diacetate (DCFDA) double stain for autophagy and ROS. Cytofluorometric acquisitions were performed as described above (MitoTracker Red, 570 nm/599 nm; DCF, 495 nm, 525 nm).

Statistical analysis

Individual samples were studied in triplicate; cells from different samples were not pooled in any experiment. The data used for statistical analysis were the means of the three repeated experiments. Statistical analysis was performed using the Statistical Package for the Social Sciences for Windows version (SPSS, Inc.). Results were reported as the mean ± 95% confidence interval (CI). Differences of means were determined by one-way analysis of variance (ANOVA) for multiple comparisons followed by least significant difference (LSD) test for two-group comparisons in multiple comparisons. The *t* test was applied to determine difference between two groups. The normality and homogeneity of variance of data were tested before statistical analysis. The nonparametric test (Karuskal Wallis) was used when the conditions for data properties were not fulfilled. *P* values less than 0.05 were considered significant. Interaction factors (age and sex) were analyzed but not included in the final model, since they were not significant.

Results

Chondrocyte ultramicro-morphology

To visualize morphological features associated with autophagy in chondrocytes, we viewed cellular ultramicroscopic structures using TEM. Normal chondrocytes exhibited massive mitochondria with normal cristae and compact, dilated endocytoplasmic reticulum (ER) to a small extent [Fig. 1(A) and (D)]. Compared with the normal samples, KBD chondrocytes appeared to exhibit serious deformation, and the nuclei were clearly distorted. The mitochondria swelled, and a great number of lysosomes were in presence in the cytoplasm [Fig. 1(B)]. The cavities could be observed in cartilage because of cell necrosis and disruption (Fig. 1 in Supplementary material). Prior to cell disintegration, nuclear cacogenesis occurred, and large numbers of glycogen deposits and

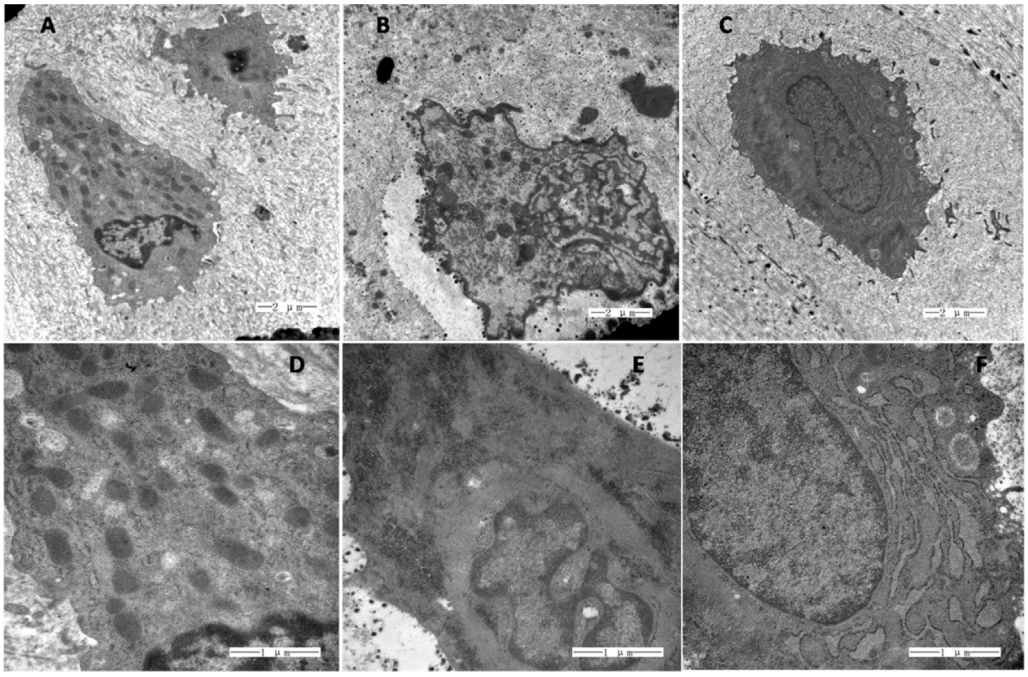

Fig. 1. Chondrocyte morphology under TEM observation (A–C, TEM × 3,000; D–F, TEM × 10,000). Chondrocytes in normal cartilage showed normal nuclear and cytoplasmic morphology such as abundant and compact mitochondria, and slightly dilated ER (A and D). KBD chondrocytes showed deformed nuclear, swelled mitochondria, and a great number of lysosomes (B). Gross microfilaments were pervasive around giant nuclei, and masses of glycogen flooding the cytoplasm (E). The main characteristics of OA chondrocytes were severely dilated ER and several degenerating lysosomes and unrecognizable organelles (C and F).

microfilaments diffused throughout the cytoplasm together with a few organelles [Fig. 1(E)]. In OA chondrocytes, the nuclei appeared normal. Lysosomes were degenerating (unrecognizable) organelles, and there were few contents and a deal of homogeneous cytoplasmic composition. Different from the normal and KBD samples, abound ER swelled and were degranulated, presenting low electron density [Fig. 1(C) and (F)]. Autophagosome was identified based on its double-membraned structure by TEM, but no autophagosome was viewed in any type of cartilage. In total, lysosomes could be seen in normal, KBD and OA cartilages, however, autophagosomes were not observed in all types of cartilage. Compared to the normal, chondrocytes in KBD cartilage showed a variety of abnormal cellular contents including nuclei, mitochondrial, glycogen deposits and microfilaments, and that OA were mainly involved on swelled ER.

Autophagic protein expression in cartilage tissue and chondrocytes

To evaluate the level of autophagic protein expression in patients with KBD and OA, Beclin1 (autophagy regulator) and LC3 (autophagy executor) in articular cartilage were detected using immunohistochemistry (IHC) (Fig. 2), together with Beclin1, LC3 and p62/SQSTM1 (LC3 interacting protein) in cultured chondrocytes using western blotting (Fig. 3).

In cartilage, Beclin1 [Fig. 2(A)] and LC3 [Fig. 2(B)] expression levels were both significantly reduced in KBD and in OA chondrocytes compared with the normal controls, and they were higher in KBD than in OA (Table I). The same trends were observed in every zone except there was no significance between the normal middle zone and the KBD middle zone. Meanwhile, these two proteins in the superficial, middle and deep zones gradually decreased in all of the normal, KBD and OA cartilages. Thus, Beclin1 and LC3 were highly expressed in normal cartilage, with overall reduced expression in KBD and OA.

In chondrocytes, endogenous Beclin1, LC3 and p62/SQSTM1 protein expression indicated autophagic levels (Fig. 3). The densitometric analysis showed significant decreases in expression of Beclin1 and LC3 in both KBD and OA chondrocytes compared with normal cells, and significantly increased expression of the two proteins in KBD compared with OA chondrocytes (Table I). The LC3-II protein level in normal and KBD chondrocytes was higher than in OA (Table I). Expression of p62 in KBD chondrocytes was increased compared with that in OA (Table I), and there were no differences between the normal cells vs KBD or OA chondrocytes.

Conclusions as a result, Beclin1 and total LC3 expression presented mostly similar patterns in normal cartilage and chondrocytes, Beclin1 and LC3 were at lower levels in both KBD and OA

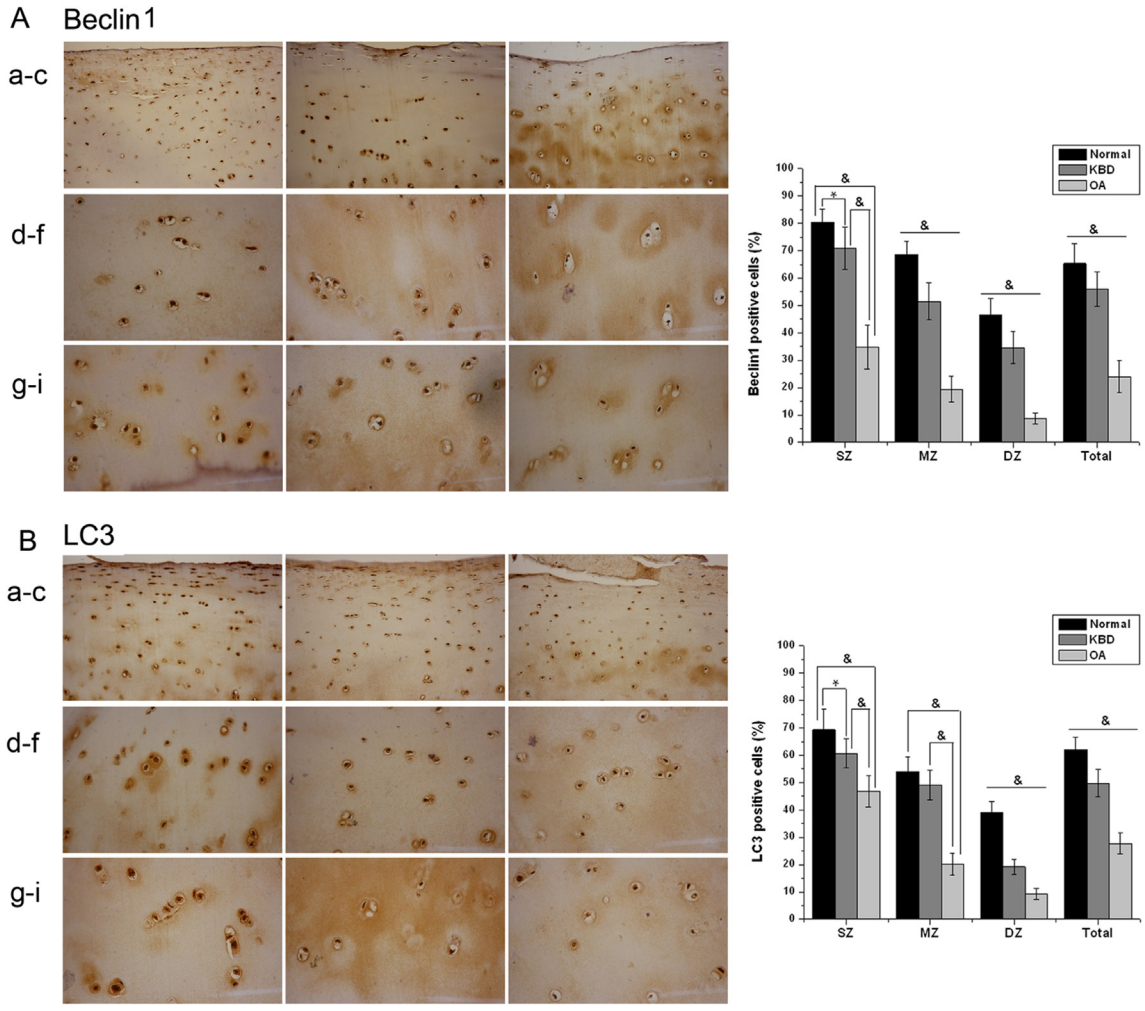

Fig. 2. Immunohistochemical localization of Beclin1 (A) and LC3 (B) in cartilage. $n = 6$ in each group. In the bars, values are the mean and SD. * = $P < 0.05$, & = $P < 0.01$. (A and B), a–c, original magnification ×200 of superficial zone (SZ) and middle zone (MZ) of normal, KBD and OA cartilage. d–f, original magnification ×400 of middle zone. g–i, original magnification ×400 of deep zone (DZ). Beclin1, $P = 0.034$ SZ of normal vs SZ of KBD; $P = 0.001$ DZ of normal vs DZ of KBD. LC3, $P = 0.032$ SZ of normal vs SZ of KBD; $P = 0.002$ SZ of KBD vs SZ of OA; $P = 0.116$ MZ of normal vs MZ of KBD. The others P values < 0.001.

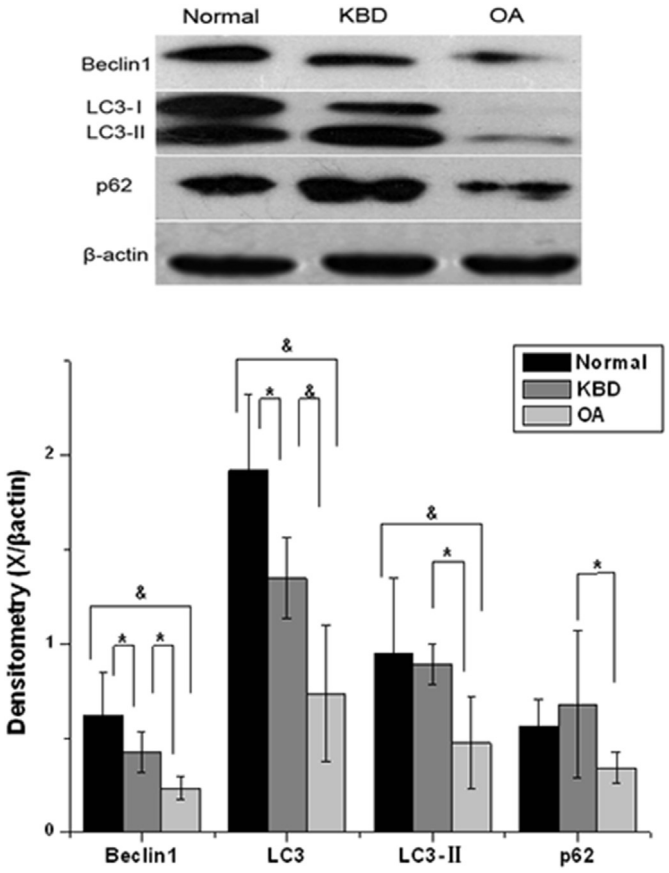

Fig. 3. Immunoblotting of cellular Beclin1, LC3, LC3-II and p62. The representative immunoblotting images of Beclin1, LC3 and p62 and the bar of densitometric analysis. $n = 6$ in each group.* = $P < 0.05$, & = $P < 0.01$. Beclin1, $P = 0.039$ Normal vs KBD; $P = 0.040$ KBD vs OA. LC3, $P = 0.010$ Normal vs KBD; $P = 0.007$ KBD vs OA. LC3-II, $P = 0.710$ Normal vs KBD; $P = 0.010$ Normal vs OA; $P = 0.020$ KBD vs OA. p62, $P = 0.430$ Normal vs KBD; $P = 0.134$ Normal vs OA; $P = 0.030$ KBD vs OA. The others P values < 0.001.

compared with the normal chondrocytes, and expression of these two proteins in KBD chondrocytes was a little higher than in OA chondrocytes. However, LC3-II, which indicates active autophagy, was higher in KBD than OA chondrocytes. Consequently, LC3 interacting protein p62 was increased in KBD chondrocytes compared with OA.

Microarray data analysis for regulated-autophagy gene profiles

The oligonucleotide microarray data were analyzed using IPA to investigate regulated-autophagy gene profiles (Fig. 4). When KBD chondrocytes were compared with normal chondrocytes, 146 autophagic genes were detected, of which 45 genes expressed different under fold change equals to 1.5 (increased expression) or 0.67 (decreased expression), including 41 genes with higher expression and four genes with lower expression. When KBD chondrocytes were compared with OA chondrocytes, 197 autophagic genes were detected, of which 92 genes expressed different under fold change equals to 1.5 or 0.67, including 62 genes with higher expression and 30 genes with lower expression. The significantly different genes and their top functions in the two analyses are presented in Tables II and III, and the associated networks are shown in Supplemental material Figs. 2 and 3. In the significant genes list, it was found that KBD was different from the normal control: there were some genes which not only participate in autophagy, but are also involved in mitochondrial function and cell death, such as BAK1, BNIP3, BNIP3L, BAX, BCL2, FOS and others. Many regulated genes and ATG were differentially expressed in KBD compared with OA chondrocytes, such as ULK1, ULK2, BECN1, BNIP3, BNIP3L, ATG10, ATG12, ATG13, ATG14 and ATG16L2. The top molecular and cellular functions in the two analyses are generally common, such as cell morphology, cellular function and maintenance, cellular assembly and organization, cell death and survival [Fig. 4(B) and (C)]. We chose five genes for quantitative RT-PCR to validate the oligonucleotide array data. The quantitative RT-PCR analyses yielded results that were consistent with the microarray data [Fig. 4(D)].

Table I
Autophagic protein expression in cartilage tissue and chondrocytes

	Normal ($n = 6$) mean (95% CI)	KBD ($n = 6$) mean (95% CI)	OA ($n = 6$) mean (95% CI)
Protein expression in cartilages using IHC (positive cell rate)			
Beclin1	0.65 (0.58–0.73)	0.56 (0.49–0.63)	0.24 (0.18–0.30)
LC3	0.62 (0.57–0.67)	0.50 (0.45–0.55)	0.27 (0.24–0.32)
Cellular protein expression using western blot (densitometry, X/β-actin)			
Beclin1	0.62 (0.38–0.86)	0.42 (0.17–0.30)	0.23 (0.17–0.30)
LC3	1.92 (1.49–2.34)	1.35 (1.12–1.57)	0.74 (1.12–1.57)
LC3-II	0.95 (0.53–1.37)	0.89 (0.78–1.00)	0.47 (0.22–0.73)
p62	0.56 (0.42–0.71)	0.68 (0.27–1.09)	0.34 (0.25–0.43)

Correlation between chondrocyte autophagy and cell death

Autophagic cell death is one type of cell death process. To estimate the correlation between autophagy and cell death, double staining of chondrocytes with MDC and PI was performed. The fluorescent images and fluorescence intensity analysis are presented in Fig. 5 and Table IV. The fluorescence intensity of MDC in chondrocytes, representing autophagy, was higher in normal chondrocytes than in KBD and OA chondrocytes. Meanwhile, the fluorescence intensity of PI showed the opposite trend. The ratios of MDC/PI (fluorescence intensity) in normal, KBD and OA chondrocytes were respectively 2.63, 1.82 and 1.35 (Fig. 5). Both KBD and OA chondrocytes showed higher apoptotic rates compared to normal control chondrocytes. After treating chondrocytes with rapamycin, apoptotic rates were decreased (Table IV).

Association between autophagy and mitochondrial function

Mitochondria are considerable organelle that participate autophagy process. Meanwhile, mitochondria play an important role in stress responses by producing ROS when damaged. So we measured the co-localization of autophagic vacuoles with mitochondria, as well as with ROS staining. The fluorescent images and fluorescence intensity analysis are presented in Fig. 6. In the three groups, rates of MDC to MitoTracker Red (fluorescence intensity) were of similar magnitude. In normal chondrocytes, the ratio of MDC to DCF (fluorescence intensity) was obviously large, reaching 3.24. However, the fluorescence intensity *per se* or the ratio in KBD chondrocytes and OA chondrocytes were similar, that were 1.69 and 1.50, respectively.

Discussion

By integrating morphological characteristics, protein expression and regulated-autophagy gene analysis, we concluded that autophagy was defective in chondrocytes from KBD and OA, but it was higher in the KBD than OA condition. Autophagy is generally regarded as a cytoprotective pathway and a potential anti-aging mechanism in cartilage, and its loss is related to OA[20,21]. A model

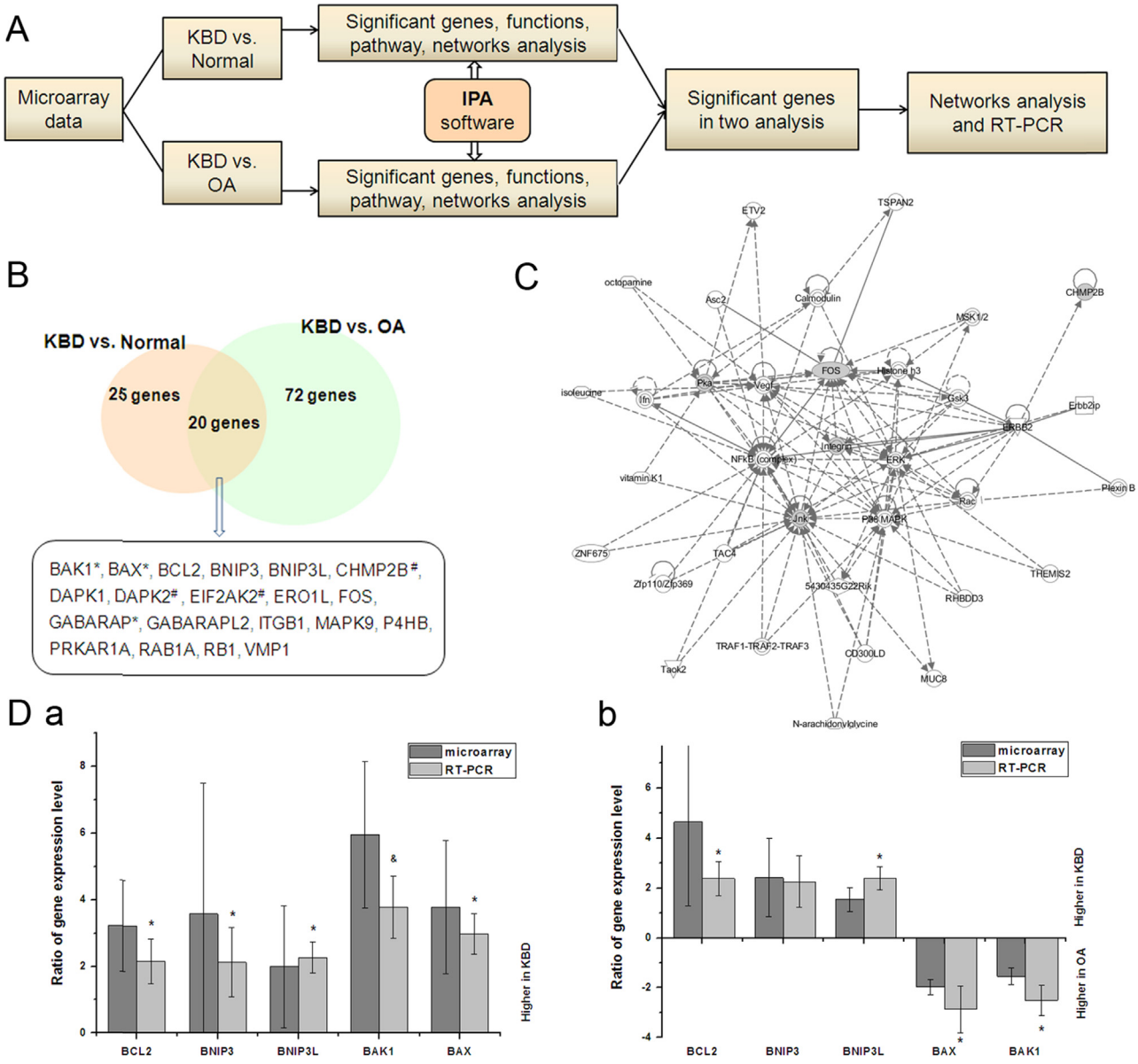

Fig. 4. The microarrays data analysis. (A) The fluidogram of microarrays data analysis. (B) The dimension of two comparisons KBD vs normal and KBD vs OA. * means increased expression when KBD vs Normal, and decreased expression when KBD vs OA; # means decreased expression when KBD vs Normal, and increased expression when KBD vs OA; no sign means increased expression when KBD vs Normal, and increased expression when KBD vs OA. (C) The network of significant genes in two comparisons analyzed by IPA. (D) Histogram showing levels of expression of five selected genes, as measured by microarray (dark gray bars: $n = 4$) and RT-PCR (light gray bars: $n = 6$). Values are the mean ± SD. *=$P < 0.05$, & = $P < 0.01$. a, KBD vs the normal. The P values of BCL2, BNIP3, BNIP3L, BAX, BAK1 were 0.045, 0.044, 0.001, 0.006, and 0.034, respectively. Ratio > 0 means gene expression level was higher in KBD. b, KBD vs OA. The P values of BCL2, BNIP3, BNIP3L, BAX, BAK1 were 0.022, 0.114, 0.035, 0.027, and 0.032, respectively. Ratio > 0 means gene expression level was higher in KBD, and Ratio < 0 means gene expression level was higher in OA.

using aging mice showed decreased expression of ULK1, Beclin1 and LC3 together with proteoglycan loss, and this correlated with an increase in the apoptosis marker poly ADP-ribose polymerase p85 (PARP p85)[13]. In contrast, some investigations showed that LC3-II levels and autophagy in chondrocytes from OA cartilage were increased compared with normal chondrocytes, indicating an adaptive response to protect cells from stresses[22].

Although no autophagosome was viewed in any type of cartilage by TEM, it may be related with the transient character and low level of autophagy. The rapid process of autophagy allows the autophagosomes to be observed in a few minutes after induction and the autolysosomes disappeare after 2 h. Meanwhile, cells rarely occur to autophagy under normal conditions, unless there are some inductors. The results showed the level of autophagy in KBD *per se* was lower than that in the normal group. However, the characteristics of chondrocytes showed swollen mitochondria and large amounts of glycogen deposits and microfilaments in the KBD chondrocytes, and dilated ER and lysosomes in the OA cells. Those might be associated with autophagic vacuoles. The formation of autophagosomes and the autophagic process are based on the isolation membrane supplied by the above-mentioned structural organelles. The ER and mitochondria contribute membranes to autophagosomes[23,24]. Prolonged ER stress induces progressive autophagy and a relative inability to utilize extracellular glucose[25]. Microtubules and mitochondria bridge with autophagic components to affect autophagosomal biogenesis and degradation by microtubule-associated protein 1S[26]. Autophagosomes are formed at random

Table II
Differentially expressed genes organized into five networks and the top functions when KBD was compared with normal chondrocytes

	Differentially expressed genes	Top functions
Network 1	BAK1, BNIP3, BNIP3L, CALCOCO2, CD46, *EIF2AK2*, EIF2AK3, GABARAP, GABARAPL2, GAPDH, MAP1LC3B, MAPK9, PRKAR1A, RB1CC1, SIRT1, TBK1, USP10, VMP1	Cell morphology, cellular function and maintenance, cellular assembly and organization
Network 2	BAX, BCL2, CAPNS1, *CTSB*, DAPK1, DDIT3, EIF4G1, ERO1L, ITGB1, ITPR1, P4HB, RAB1A,	Cell death and survival, cellular assembly and organization, cell morphology
Network 3	ATG4C, *CHMP2B*, KLHL24, PEX3, RAB11A, TM9SF1, WDR45L	Cell signaling, cellular function and maintenance, infectious disease
Network 4	*DAPK2*, FOS, KIF5B, SESN2	Cellular assembly and organization, cellular function and maintenance, cancer
Network 5	CTSD, MYC, NCKAP1, RB1	Cell death and survival, cell cycle, connective tissue development and function

In italics are the genes with low expression. The genes presented in the table were differentially expressed, and all molecules in the networks are shown in the Supplementary materials.

Table III
Differentially expressed genes organized into the top five networks and the top functions when KBD was compared with OA chondrocytes

	Differentially expressed genes	Top functions
Network 1	ATG10, ATG12, *ATG13*, ATG14, ATG16L2, BECN1, BNIP3, BNIP3L, CD46, FKBP1A, FKBP1B, *GABARAP*, *GABARAPL1*, GABARAPL2, GOPC, MAP1LC3C, PIK3C3, PINK1, *ULK1*, ULK2, WIPI1	Cell morphology, cellular function and maintenance, cellular assembly and organization
Network 2	BCL2, *BCL2L1*, CASP1, *CDKN1A*, CHMP2B, ERBB2, HSPA8, IKBKB, PTEN, *RELA*, *SQSTM1*, WDFY3	Cell morphology, cellular function and maintenance, cell death and survival
Network 3	*APOL1*, *BAX*, CAMKK2, CAPN1, CAPN2, DAPK2, *EEF2*, ERN1, ERO1L, RPS6KB1, *SERPINA1*, TSC1	Cell morphology, cellular function and maintenance, protein synthesis
Network 4	*ATF4*, DAPK1, EIF2AK2, FOS, *MAPK3*, MAPK9, *NPC1*, RAB33B, ST13	Cell death and survival, cell cycle, protein synthesis
Network 5	CHMP4B, CXCR4, EGFR, *GNB2L1*, ITGB1, NRG1, PRKAR1A	Cellular movement, cancer, cell-to-cell signaling and interaction
Network 6	*BAK1*, BIRC5, CDKN2A, *MAP2K7*, *PELP1*, RB1, *STK11*	Cell death and survival, cell cycle, cell morphology
Network 7	CCL2, *DIRAS3*, *HSP90AB1*, MBTPS2, *TP53*, VMP1, *WDR45B*	Cell death and survival, cellular compromise, cell cycle
Network 8	BID, CASP8, CFLAR, FADD, LAMP2, PEA15, VMP1	Cell death and survival, embryonic development, liver necrosis/cell death
Network 9	*BAG1*, *CLN3*, DLC1, *HSPB8*, *NFKB1*, *PPP1R15A*	Protein synthesis, cellular development, cellular growth and proliferation
Network 10	CAPN10, ITGA6, P4HB, RAB1A	Cellular assembly and organization, cellular development, cellular growth and proliferation
Network 11	*RAB24*	Cancer, cellular development, cellular growth and proliferation

In italics are the genes with low expression. The genes presented in the table were differentially expressed, and all molecules in the networks are shown in the Supplementary materials.

locations in the cell, but after completion they are transported directionally toward the nucleus, driven by the dynein motor, and fuse with endosomes or lysosomes[27]. Microtubules serve to transport mature autophagosomes and bring autophagosomes and lysosomes together for fusion[28]. The glycogen deposit accumulations indicated abnormalities in glucose utilization and energy homeostasis in KBD chondrocytes. In addition, autophagy is an important contributor to the regulation of cellular metabolic capabilities[29]. It is activated in response to metabolic stress, and supports the ability of mammalian cells to withstand nutrient deprivation. In defective autophagy, chondrocytes are unable to either provide internal nutrients or to provide an essential means of remodeling and refreshing cells[20].

In the differentially expressed gene sets, there were several such as BAK1, BNIP3, BNIP3L, BAX, BCL2 and FOS, discovered either in the comparison of KBD and normal chondrocytes or KBD and OA chondrocytes, that not only participate in autophagy but are also involved in mitochondrial function and cell death. This indicated the existence of overlap among autophagy, mitochondrial function and cell death in KBD and OA. Beclin 1 can be inhibited by binding to BCL-2 and BCL-X_L[30,31]. BNIP3L/NIX and BNIP3 are activated under hypoxia, and may cause mitophagy[32]. Many regulated genes and autophagy genes (ATG) such as ULK1, ULK2, BECN1, BNIP3, BNIP3L, ATG10, ATG12, ATG13, ATG14 and ATG16L2 were differentially expressed in KBD compared with OA chondrocytes. ATG13 combines ATG17 and mTOR to regulate the induction of autophagy. BECN1, also named Beclin1, regulates the vesicle nucleation process in the early stage of autophagy. ATG10, ATG12 and ATG 16 are involved in the two ubiquitin-like conjugation systems, in which Atg12 covalently conjugates to Atg5 with the help of ATG7 and ATG10, which are part of the vesicle elongation phase of autophagosome formation[33]. Knockdown of ATG5, ATG10 and ATG12 by RNAi can inhibit autophagy followed by alteration in cell death rates[34].

Alterations in autophagy are linked to multiple physiological changes and degenerative diseases. Accumulation of damaged mitochondria is observable in KBD chondrocytes, and mitochondrial function is altered[6]. The specific autophagic elimination of mitochondria (mitophagy) is related to mitochondrial dysfunction, a targeted defense against oxidative stress and aging[35]. Regulated morphology of mitochondria determines the fate of cells during autophagy, such that elongated mitochondria are spared from autophagic degradation and increased activity of energy maintenance; and conversely, when elongation is blocked, mitochondria consume ATP and precipitate starvation-induced death[36]. A review also indicated that an axis of mitochondria-autophagy-inflammation-cell death might contribute to multiple aging-associated pathologies[37]. Loss of autophagy results in accumulation of damaged mitochondria, which promotes inflammatory responses and cell death which are otherwise limited by autophagy. ROS was produced by damaged mitochondria or in aged cells under normal growth conditions, whereas autophagy is compromised in age-related disorders such as OA[38,39]. ROS was revealed as a signaling molecule in autophagic pathways, leading to either cell survival or death. Enhanced ROS can create an oxidative gradient, which favors pro-apoptotic mitochondrial outer membrane permeabilization (MOMP) as well as stimulating the activity of cysteine protease Atg4[40,41]. Therefore, the fate of the cell under stress is decided by multiple connections between the apoptotic and autophagic processes, and mitochondrial function. Experimental models demonstrated that cell death of chondrocytes in OA resulted from a combination of apoptosis and autophagy[42].

By monitoring autophagosome formation, autophagic gene profiles and protein expression, we suggest that autophagy was

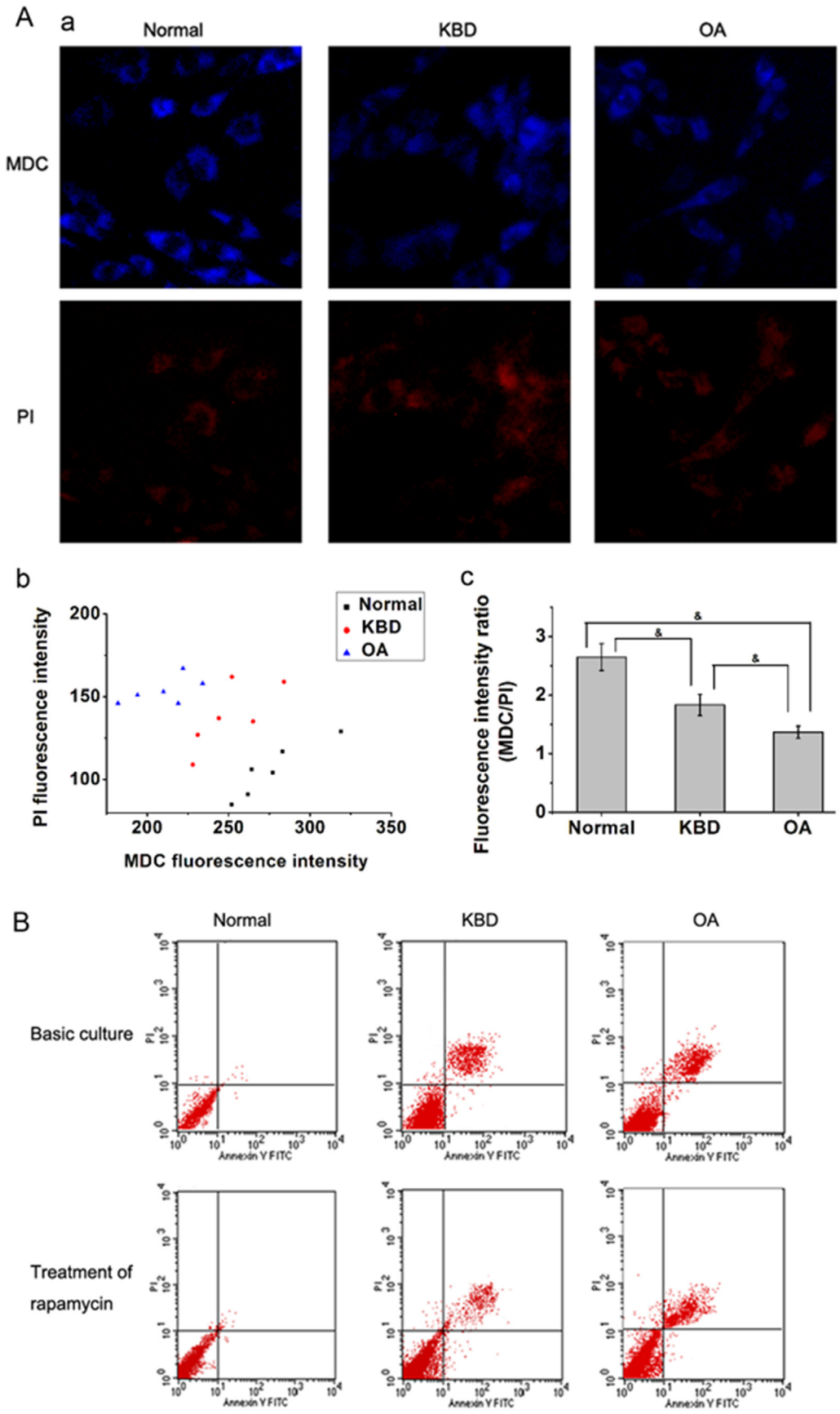

Fig. 5. Measurements of autophagy and cell death. $n = 6$ in each group. (A) Fluorescence measurements of autophagic level (MDC fluorescence) and cell death (PI fluorescence). a, The image of MDC and PI fluorescence stain. MDC, emitting in blue; PI, emitting in red. b, the scatterplot of fluorescence intensity. Each plot presents one sample. c, the bar graph of fluorescence intensity ratio. The ratio is fluorescence intensity of MDC to PI. $P < 0.001$ normal vs KBD, normal vs OA and KBD vs OA. (B) Chondrocyte apoptosis was measured by FCM. The three detected samples above were the normal, KBD and OA chondrocytes, respectively, and the three below were corresponding chondrocytes with rapamycin treatment.

Table IV
Apoptosis rate of chondrocytes under basic culture or with rapamycin treatment

	Normal ($n = 6$) mean (95% CI)	KBD ($n = 6$) mean (95% CI)	OA ($n = 6$) mean (95% CI)	*P* value
Basic culture (A)	3.43 (2.54–4.31)	18.14 (15.16–21.12)	20.51 (17.19–23.83)	<0.001*
With rapamycin (B)	3.42 (2.87–3.97)	13.86 (11.3–16.41)	16.39 (13.98–18.81)	<0.001†
Change (A–B)	0.01 (−0.45–0.44)	4.28 (3.49–5.07)	4.12 (3.01–5.22)	0.001‡
P value	0.985	<0.001	<0.001	

$n = 6$.
* $P < 0.001$ Normal vs KBD and Normal vs OA; it is not significance between KBD and OA ($P = 0.121$).
† $P < 0.001$ Normal vs KBD and Normal vs OA; $P = 0.040$ KBD vs OA.
‡ $P < 0.001$ Normal vs KBD and Normal vs OA; it is not significance between KBD and OA ($P = 0.723$).

defective in KBD, but higher than that in OA. The results also showed insufficient autophagy might be associated with apoptosis and mitochondrial change in KBD and OA. It will become a challenging endeavor for future investigations to determine how autophagy, mitochondria and cell death cross-talk in the pathology of KBD.

Author contributions

All authors were critically involved in drafting or revising the article, and all authors approved the final version to be published. Cuiyan Wu had full access to all of the experiments, integrity of the data and accuracy of data analysis in the study. Study was designed by Cuiyan Wu and Xiong Guo. The collection of cartilage samples was done by Yi Li and Peng Xu. Jingjing Zheng and Hu Shan participated in the experimental process. Xiao Yao was responsible for the analysis of data.

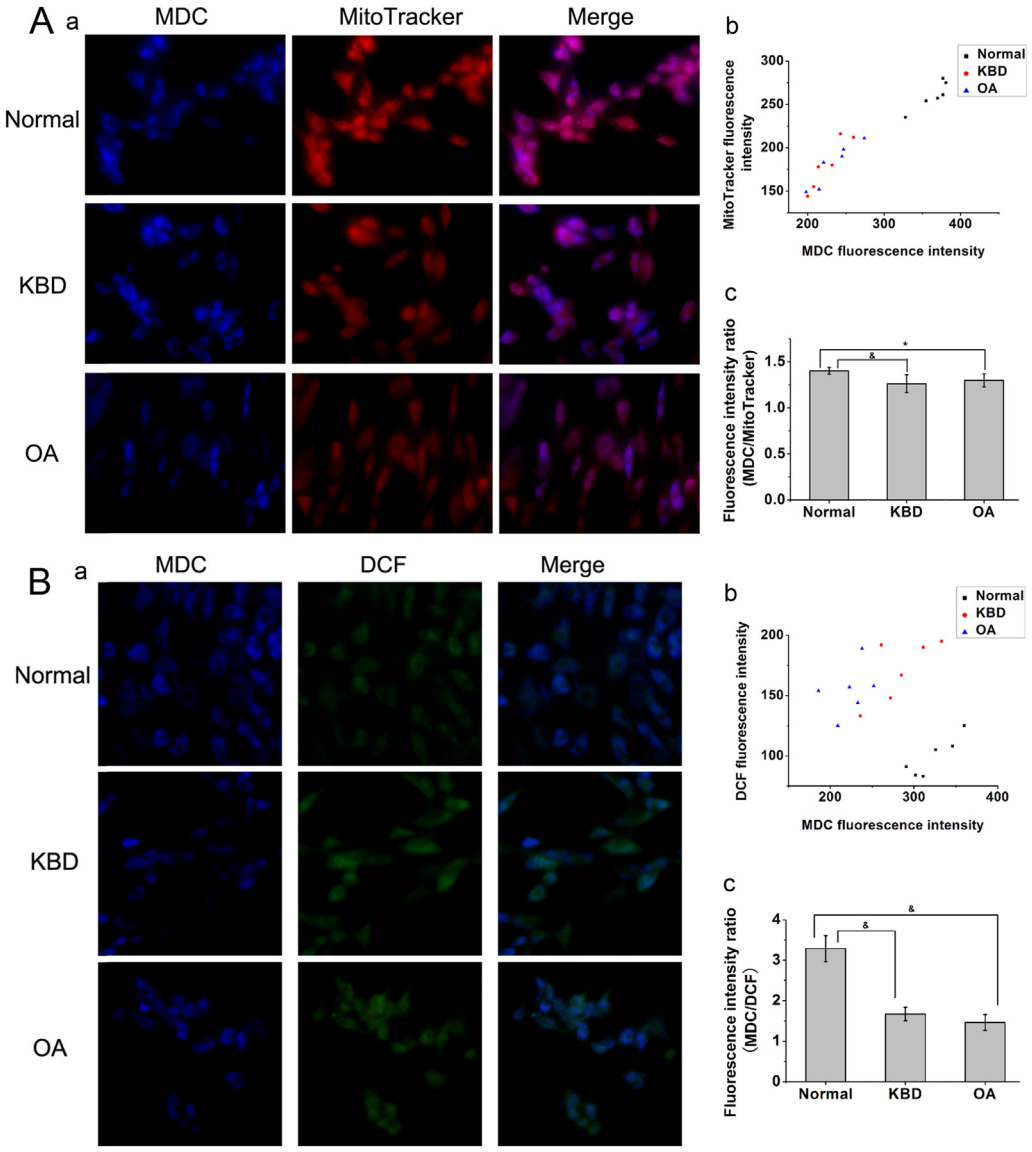

Fig. 6. Indicators of autophagy and mitochondrial function. $n = 6$ in each group. (A) a, Co-localization of autophagic vacuoles (MDC blue fluorescence) with mitochondria (MitoTracker Red fluorescence). b, the scatterplot of fluorescence intensity. Each plot presents one sample. c, the bar graph of fluorescence intensity ratio. The ratio is fluorescence intensity of MDC to MitoTracker. $P = 0.005$ normal vs KBD; $P = 0.025$ normal vs OA; $P = 0.409$ KBD vs OA. (B) Double staining of autophagy (MDC blue fluorescence) and ROS (DCF green fluorescence). b, the scatterplot of fluorescence intensity. Each plot presents one sample. c, the bar graph of fluorescence intensity ratio. The ratio is fluorescence intensity of MDC to DCF. $P < 0.001$ normal vs KBD; $P < 0.001$ normal vs OA; $P = 0.253$ KBD vs OA.

Funding source
This work was supported by the National Natural Scientific Foundation of China (30972556); and "13115" Major program on Technology Science Innovation Project of Shaanxi Province (2009ZDKG-79).

Conflicts of interest
None declared.

Acknowledgments

We thank all the donators of cartilages and the surgeons and nursing staff in Hong Hui Hospital in the collection of cartilage specimens. Supported by the National Natural Scientific Foundation of China (30972556) and "13115" Major program on Technology Science Innovation Project of Shaanxi Province (2009ZDKG-79). We thank Professor Mikko Lammi in Eastern Finlan University for his comments and revisions.

Supplementary data

Supplementary data related to this article can be found at http://dx.doi.org/10.1016/j.joca.2014.08.010.

References

1. Hinsenkamp M. Kashin-Beck disease. Int Orthop 2001;25. 133–133.
2. Yamamuro T. Kashin-Beck disease: a historical overview. Int Orthop 2001;25:134–7.
3. Cao J, Li S, Shi Z, Yue Y, Sun J, Chen J, *et al.* Articular cartilage metabolism in patients with Kashin–Beck disease: an endemic osteoarthropathy in China. Osteoarthritis Cartilage 2008;16: 680–8.
4. Wang S, Guo X, Ren F, Zhang Y, Zhang Z, Zhang F, *et al.* Comparison of apoptosis of articular chondrocytes in the pathogenesis of Kashin-Beck disease and primary osteoarthritis. Zhongguo Yi Xue Ke Xue Yuan Xue Bao. Acta Academiae Medicinae Sinicae 2006;28:267.
5. Wang SJ, Guo X, Zuo H, Zhang YG, Xu P, Ping ZG, *et al.* Chondrocyte apoptosis and expression of Bcl-2, Bax, Fas, and iNOS in articular cartilage in patients with Kashin-Beck disease. J Rheumatol 2006;33:615–9.
6. Liu JT, Guo X, Ma WJ, Zhang YG, Xu P, Yao JF, *et al.* Mitochondrial function is altered in articular chondrocytes of an endemic osteoarthritis, Kashin-Beck disease. Osteoarthritis Cartilage 2010;18:1218–26.
7. Wang WZ, Guo X, Duan C, Ma WJ, Zhang YG, Xu P, *et al.* Comparative analysis of gene expression profiles between the normal human cartilage and the one with endemic osteoarthritis. Osteoarthritis Cartilage 2009;17:83–90.
8. Ma WJ, Guo X, Liu JT, Liu RY, Hu JW, Sun AG, *et al.* Proteomic changes in articular cartilage of human endemic osteoarthritis in China. Proteomics 2011;11:2881–90.
9. Shapiro IM, Adams CS, Freeman T, Srinivas V. Fate of the hypertrophic chondrocyte: microenvironmental perspectives on apoptosis and survival in the epiphyseal growth plate. Birth Defects Res C Embryo Today 2005;75:330–9.
10. Srinivas V, Shapiro IM. Chondrocytes embedded in the epiphyseal growth plates of long bones undergo autophagy Ppior to the induction of osteogenesis. Autophagy 2006;2: 215–6.
11. Rubinsztein DC, Mariño G, Kroemer G. Autophagy and aging. Cell 2011;146:682–95.
12. Loeser RF. Aging and osteoarthritis. Curr Opin Rheumatol 2011;23:492.
13. Caramés B, Taniguchi N, Otsuki S, Blanco FJ, Lotz M. Autophagy is a protective mechanism in normal cartilage, and its aging-related loss is linked with cell death and osteoarthritis. Arthritis Rheum 2010;62:791–801.
14. Srinivas V, Bohensky J, Shapiro IM. Autophagy: a new phase in the maturation of growth plate chondrocytes is regulated by HIF, mTOR and AMP kinase. Cells Tissues Organs 2008;189: 88–92.
15. Bohensky J, Leshinsky S, Srinivas V, Shapiro IM. Chondrocyte autophagy is stimulated by HIF-1 dependent AMPK activation and mTOR suppression. Pediatr Nephrol 2010;25: 633–42.
16. Bohensky J, Terkhorn SP, Freeman TA, Adams CS, Garcia JA, Shapiro IM, *et al.* Regulation of autophagy in human and murine cartilage: hypoxia-inducible factor 2 suppresses chondrocyte autophagy. Arthritis Rheum 2009;60:1406–15.
17. Roach H, Aigner T, Kouri J. Chondroptosis: a variant of apoptotic cell death in chondrocytes? Apoptosis 2004;9: 265–77.
18. Levine B, Kroemer G. Autophagy in the pathogenesis of disease. Cell 2008;132:27–42.
19. Duan C, Guo X, Zhang X-D, Yu H-J, Yan H, Gao Y, *et al.* Comparative analysis of gene expression profiles between primary knee osteoarthritis and an osteoarthritis endemic to Northwestern China, Kashin-Beck disease. Arthritis Rheum 2010;62:771–80.
20. Lotz MK, Caramés B. Autophagy and cartilage homeostasis mechanisms in joint health, aging and OA. Nat Rev Rheumatol 2011;7:579–87.
21. Caramés B, Taniguchi N, Seino D, Blanco FJ, D'Lima D, Lotz M. Mechanical injury suppresses autophagy regulators and pharmacologic activation of autophagy results in chondroprotection. Arthritis Rheum 2012;64:1182–92.
22. Sasaki H, Takayama K, Matsushita T, Ishida K, Kubo S, Matsumoto T, *et al.* Autophagy modulates osteoarthritis-related gene expression in human chondrocytes. Arthritis Rheum 2012;64:1920–8.
23. Ylä-Anttila P, Vihinen H, Jokitalo E, Eskelinen E-L. 3D tomography reveals connections between the phagophore and endoplasmic reticulum. Autophagy 2009;5:1180–5.
24. Hailey DW, Rambold AS, Satpute-Krishnan P, Mitra K, Sougrat R, Kim PK, *et al.* Mitochondria supply membranes for autophagosome biogenesis during starvation. Cell 2010;141: 656–67.
25. Kim I, Xu W, Reed JC. Cell death and endoplasmic reticulum stress: disease relevance and therapeutic opportunities. Nat Rev Drug Discov 2008;7:1013–30.
26. Xie R, Nguyen S, McKeehan K, Wang F, McKeehan WL, Liu L. Microtubule-associated protein 1S (MAP1S) bridges autophagic components with microtubules and mitochondria to affect autophagosomal biogenesis and degradation. J Biol Chem 2011;286:10367–77.
27. He C, Klionsky DJ. Regulation mechanisms and signaling pathways of autophagy. Annu Rev Genet 2009;43:67.
28. Fass E, Shvets E, Degani I, Hirschberg K, Elazar Z. Microtubules support production of starvation-induced autophagosomes but not their targeting and fusion with lysosomes. J Biol Chem 2006;281:36303–16.
29. Rabinowitz JD, White E. Autophagy and metabolism. Science 2010;330:1344–8.
30. Levine B, Sinha SC, Kroemer G. Bcl-2 family members: dual regulators of apoptosis and autophagy. Autophagy 2008;4: 600–6.

31. Erlich S, Mizrachy L, Segev O, Lindenboim L, Zmira O, Adi-Harel S, *et al*. Differential interactions between Beclin 1 and Bcl-2 family members. Autophagy 2007;3:561–8.
32. Novak I, Kirkin V, McEwan DG, Zhang J, Wild P, Rozenknop A, *et al*. Nix is a selective autophagy receptor for mitochondrial clearance. EMBO Reports 2009;11:45–51.
33. Maiuri MC, Zalckvar E, Kimchi A, Kroemer G. Self-eating and self-killing: crosstalk between autophagy and apoptosis. Nat Rev Mol Cell Biol 2007;8:741–52.
34. Crighton D, Wilkinson S, O'Prey J, Syed N, Smith P, Harrison PR, *et al*. DRAM, a p53-induced modulator of autophagy, is critical for apoptosis. Cell 2006;126:121–34.
35. Lemasters JJ. Selective mitochondrial autophagy, or mitophagy, as a targeted defense against oxidative stress, mitochondrial dysfunction, and aging. Rejuvenation Res 2005;8:3–5.
36. Gomes LC, Di Benedetto G, Scorrano L. During autophagy mitochondria elongate, are spared from degradation and sustain cell viability. Nat Cell Biol 2011;13:589–98.
37. Green DR, Galluzzi L, Kroemer G. Mitochondria and the autophagy–inflammation–cell death axis in organismal aging. Science 2011;333:1109–12.
38. Blanco FJ, Rego I, Ruiz-Romero C. The role of mitochondria in osteoarthritis. Nat Rev Rheumatol 2011;7:161–9.
39. Fukuda K. Progress of research in osteoarthritis. Involvement of reactive oxygen species in the pathogenesis of osteoarthritis. Clin Calcium 2009;19:1602.
40. Scherz-Shouval R, Shvets E, Fass E, Shorer H, Gil L, Elazar Z. Reactive oxygen species are essential for autophagy and specifically regulate the activity of Atg4. EMBO J 2007;26:1749–60.
41. Scherz-Shouval R, Elazar Z. ROS, mitochondria and the regulation of autophagy. Trends Cell Biol 2007;17:422–7.
42. Almonte-Becerril M, Navarro-Garcia F, Gonzalez-Robles A, Vega-Lopez M, Lavalle C, Kouri J. Cell death of chondrocytes is a combination between apoptosis and autophagy during the pathogenesis of osteoarthritis within an experimental model. Apoptosis 2010;15:631–8.